Available online at www.sciencedirect.com
SCIENCE DIRECT®
Scripta Materialia 52 (2005) 393–397
Scripta MATERIALIA
www.actamat-journals.com

Feasibility assessment of self-grading metallic bond coat alloys for EBCs/TBCs to protect Si-Based ceramics

M.P. Brady [a,*], B.L. Armstrong [a], H.T. Lin [a], M.J. Lance [a], K.L. More [a], L.R. Walker [a], F. Huang [b], M.L. Weaver [b]

[a] *Department of Metals and Ceramics, Oak Ridge National Laboratory, ms 6115, Oak Ridge, TN 37831-6115, USA*
[b] *University of Alabama, Tuscaloosa, AL 35487-0202, USA*

Received 29 July 2004; received in revised form 6 October 2004; accepted 18 October 2004
Available online 11 November 2004

Abstract

A sputtered γ (TiAl) + Laves TiAlCr coating formed an adherent Al_2O_3 scale on SN 282 Si_3N_4 when oxidized. A Ti–N rich layer was formed at the TiAlCr–Si_3N_4 interface, which effectively resulted in beneficial local Al enrichment underneath the growing Al_2O_3 scale, rather than detrimental Al loss to the substrate.
© 2004 Acta Materialia Inc. Published by Elsevier Ltd. All rights reserved.

Keywords: Silicon nitride; Oxidation; Coating; Surface alloying; Environmental barrier coatings (EBC); Thermal barrier coatings (TBC)

1. Introduction

Silicon nitride, silicon carbide, and related Si-based monolithic and composite materials are candidates for a variety of high-temperature applications. The environmental durability of these materials is based on the establishment of a continuous, protective SiO_2 surface layer. However, for applications such as gas turbine components, which typically involve high gas flow rates and exposure to environments containing water vapor, the ability of SiO_2 to act as a protective coating can be severely compromised due to volatilization and accelerated oxidation [1–8]. Environmental barrier coatings (EBCs) are being pursued to mitigate this problem. The most successful EBCs to date have been based on a multi-layered analog to thermal barrier coatings (TBCs), with a BSAS (BaO–SrO–Al_2O_3–SiO_2) top coat, a mullite-based intermediate coat, and Si bond coats [2,4,6]. These materials have exhibited promising behavior as protective coatings for ceramic composite combustor liners in long-term land-based gas turbine tests (>15,000 h at 1200 °C), however the observed rates of EBC degradation are still too rapid to achieve the desired 25,000–40,000 h lifetimes for these applications [4,7].

The purpose of this work was to explore the possibility of using metallic alloys as protective coatings for Si-based ceramics. This approach is potentially amenable to the formation of a wide range of oxide phases from the precursor metallic coating alloy, including complex (ternary and higher order) oxide phases as well as duplex (multi-phase) scales [9]. For a proof of principle exploration, an alloy that formed Al_2O_3 (α) was selected for this study. Al_2O_3-formers are attractive as volatility barriers due to a combination of low scaling rates and relatively good stability in water vapor environments [10], and are estimated to offer sufficiently low growth rates for the desired 25,000–40,000 h lifetimes up to ~1100–1150 °C; the exact upper temperature limit dependent on factors such as thermal cycling conditions, coating/

* Corresponding author. Tel.: +1 865 574 5153; fax: +1 865 241 0215.
E-mail address: bradymp@ornl.gov (M.P. Brady).

1359-6462/$ - see front matter © 2004 Acta Materialia Inc. Published by Elsevier Ltd. All rights reserved.
doi:10.1016/j.scriptamat.2004.10.024

component thickness, Al reservoir, etc. (The temperature limit estimate is based on literature data, for example, 0.1 cm thick Zr-doped Ni-50Al at.% exhibited an estimated lifetime of only 10,000 h at ~1200 °C [11].) An additional 75–150 °C higher operating temperature may be achieved if used in conjunction with a ceramic topcoat to reduce the effective metal temperature, i.e. a TBC/EBC. The main drawback of Al_2O_3 is that its coefficient of thermal expansion (CTE) is significantly higher than that of Si_3N_4 and SiC (~9 vs $\sim 3 \times 10^{-6}$/°C), and, further, the CTE of the metallic precursor alloy ($> \sim 12 \times 10^{-6}$/°C) would be significantly higher than that of the Al_2O_3. These CTE mismatches can lead to scale cracking, spallation, and ultimately, coating failure.

An advantage of metallic-based precursor compositions over direct deposition of Al_2O_3 (or other oxides) is the opportunity to design the alloy to react (interdiffuse) with the substrate in a manner such that a self-graded, potentially adherent coating will form. Depending upon the initial thickness and compositional makeup of the coating, it may also be possible to retain a reservoir of an Al-rich phase underneath the scale to permit local healing of the Al_2O_3 in the event of scale cracking.

Conventional bond coat compositions based on Fe or Ni are not considered attractive options because Fe and Ni react with Si to form low melting point ($\leqslant$~1200 °C) eutectics. They also are less thermodynamically stable with nitrogen and carbon than Si, and are therefore unlikely to self grade in the desired manner. Therefore, an Al_2O_3-forming Ti-based alloy, 37Ti–51Al–12Cr atomic percent (at.%) (TiAlCr) was chosen for evaluation. This alloy was originally designed as a protective coating for γ-based titanium aluminide alloys in the 800–1000 °C range [12], however it appears ideal for a proof of principle assessment of self-grading, metallic protective-scale forming alloys as EBCs for Si-based ceramics. The lowest melting eutectic in the Ti–Si system is in the range of 1330 °C, and, further, carbides and nitrides of Ti are more thermodynamically stable than those of Si. The goal of this effort was to explore the interaction of the TiAlCr coating with Si_3N_4 under oxidizing conditions and to assess the potential to form an adherent, self-graded protective Al_2O_3-based layer.

2. Experimental

Coupons of SN282 Si_3N_4 (Kyocera; Kyoto, Japan) of dimensions $\sim 26 \times 12 \times 3$ mm were procured for study. The TiAlCr alloy was applied as a coating by magnetron sputtering of a 37Ti–51Al–12Cr master target alloy to a nominal thickness of 8–10 μ on the main coupon faces, 4 μ on the long (edge) faces, and 2 μ on the short (edge) faces. Two oxidation exposures were conducted: three 100 h cycles (air cooling) at 1000 °C open to ambient "laboratory" air and three 100 h cycles (air cooling) at 1000 °C in filtered compressed dry air, for which the latter 2, 100 h cycles 20 vol.% of water vapor was added. Control samples of arc-cast TiAlCr (12 mm diameter, 1 mm thick) were oxidized alongside the coated coupons. As the purpose of these experiments were strictly proof-of-principle of the metallic coating approach, the relatively low 1000 °C oxidation temperature was used to avoid potential complications arising from possible instability of the γ TiAl + Laves $Ti(Cr,Al_2)$ structure of TiAlCr above ~1100 °C [13,14]; such phase transformations can likely be modified through alloy design.

The microstructures of the oxidized samples were characterized using scanning electron microscopy (SEM) and electron probe microanalysis (EPMA) using pure element standards for Al, Cr, Si, and Ti; a TiN standard for N; and an Al_2O_3 standard for O. All EPMA measurements are reported in at.%. The interface between the coating and the Si_3N_4 was also examined by cross-section scanning transmission electron microscopy (STEM). The stress states of the Al_2O_3 scales were determined at room temperature by photo-stimulated luminescence spectroscopy (PSLS) [15,16].Measurements were made using a Raman microprobe configured to operate as a single-stage spectrograph with an argon ion laser operating at 5145 Å with an output power of 100 mW. The attached microscope was defocused to produce a spot size of ~100 μ on the coupon surface thereby decreasing the laser heating while collecting signal from a larger region.

3. Results and discussion

The Al_2O_3-based scales formed on the TiAlCr-coated SN282 and the cast TiAlCr remained adherent, with no evidence of spallation over the course of the three 100 h screening cycle exposure in air and air + 20% H_2O. No significant differences in the oxidation kinetics between coated TiAlCr and cast TiAlCr were evident, nor were there any significant effects of the introduction of 20% H_2O on oxidation kinetics (Fig. 1). Surface SEM did, however, reveal the presence of cracks in the Al_2O_3 scale formed on the TiAlCr coated SN 282 in both air and air + 20% H_2O (Fig. 2b). Similar cracks were not evident in the Al_2O_3 formed on the cast TiAlCr (Fig. 2a).

PSLS stress measurements of the Al_2O_3 scales are summarized in Table 1. Large compressive stresses on the order of −2800 MPa were observed for the cast TiAlCr samples, while an order of magnitude lower, but still compressive stress was observed on the TiAlCr coated SN 282 samples. This reduced level of compressive stress is consistent with the observed cracks, which likely provided stress relief.

A cross-section SEM image of the TiAlCr coated SN 282 after oxidation is shown in Fig. 3. No differences

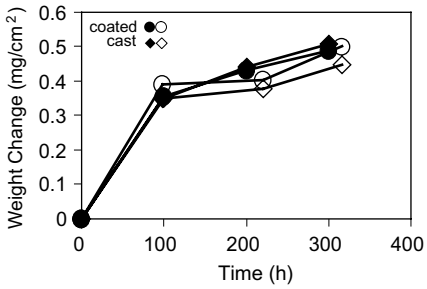

Fig. 1. Oxidation data for 37Ti–51Al–12Cr coated SN282 and cast 37Ti–51Al–12Cr control coupons at 1000 °C in air. At each data point the samples were air cooled to room temperature, weighed, and returned to the furnace (inserted at temperature). The open data points are for exposure in "laboratory" air of nominal 50% daily humidity, and the filled data points are the runs in which the second and third 100 h cycles were conducted in air + 20% water vapor.

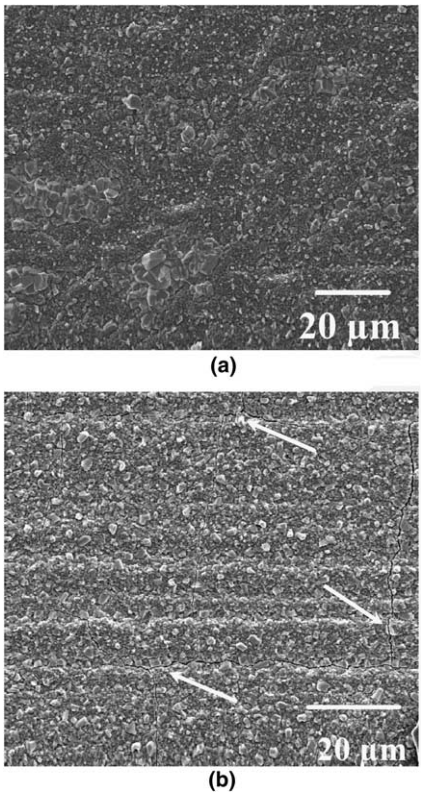

Fig. 2. Plan-view SEM images of the Al_2O_3 scale formed on (a) cast 37Ti–51Al–12Cr and (b) 37Ti–51Al–12Cr coated SN282 after three 100 h cycles at 1000 °C in air (cracks marked by arrows). Similar microstructures were observed in the air + 20% water vapor exposures.

Table 1
PSLS stress measurements of the Al_2O_3 scales formed by Ti–51Al–12Cr

Sample	Average biaxial stress (MPa): air	Average biaxial stress (MPa): air + 20% H_2O
Ti–51Al–12Cr coated SN 282	−337 ± 18	−223 ± 39
Cast Ti–51Al–12Cr	−2893 ± 21	−2727 ± 29

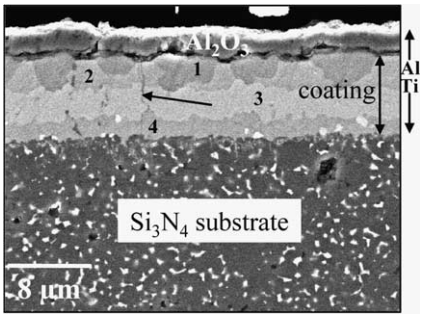

Fig. 3. SEM secondary electron cross-section image of the main faces of the 37Ti–51Al–12Cr coated SN282 coupon after the three 100 h cycle exposures at 1000 °C in air. The arrows point to cracks within the coating layer. A similar microstructure was observed in air + 20% H_2O. (1) 65Al–23Ti–11Cr–1O; (2) 60Al–34Cr–5.5Ti–0.5Si; (3) (35–42)Ti–(24–25)Si–(19–25)Cr–8Al–(0–14)N; (4) (40–60)Ti–(12–40)N–(18–25)Al–(1–2)Si,Cr.

were evident between the air and air + 20% H_2O exposures under the conditions studied. The oxidized microstructures consisted of a continuous Al_2O_3 scale overlying a three-layer structure. The layer directly underneath the Al_2O_3 consisted of a two-phase mixture of an Al–Ti–Cr rich phase (point 1, Fig. 3) of average composition 65Al–23Ti–11Cr–1O (the oxygen was likely an artifact of overlap with the Al_2O_3 scale), consistent with the τ $L1_2$ phase [17], and an Al–Cr intermetallic-based phase (point 2) of average composition 60Al–34Cr–5.5Ti–0.5Si (observed only in some coating regions examined). The second layer (point 3) consisted of a Ti-rich phase of composition in the range of (35–42)Ti–(24–25)Si–(19–25)Cr–8Al–(0–14)N, The third layer (point 4), located at the coating–SN282 interface, was a Ti–Al–N based phase of composition in the range (40–60)Ti–(12-40)N–(18–25)Al–(1–2)Si,Cr. The ranges of composition for points 3 and 4 are a byproduct of the uncertainty in the compositional analysis of Ti and N rich phases due to Ti–L and N–K EDS peak overlap (these data should therefore be considered semiquantitative). Although some cracks were evident in the coating layer (the CTEs of the metallic phases are higher than that of the substrate Si_3N_4), there was no evidence of SiO_2 formation or oxygen penetration beyond the outer Al_2O_3 layer by EDS/EPMA analysis, nor was there evidence of significant Al diffusion into the substrate (Al was not detected within a few microns of the Si_3N_4—coating interface).

A cross-section dark-field STEM image of the Si_3N_4/coating interface after short term cyclic exposure is shown in Fig. 4 with areas (layers) analyzed by EDS labeled 1, 2, and 3 on the image. Scanning TEM analysis revealed the complex nature (additional layers) within the interfacial region. The sub-micron coating layer labeled region 1 in Fig. 4 corresponds directly with region 4 labeled in Fig. 3 and had a composition of $\sim$ 2Ti:1Al. Another thin ($\sim$ 1 µm), acicular-grained, single grain-thickness layer (labeled 2 in Fig. 4), which

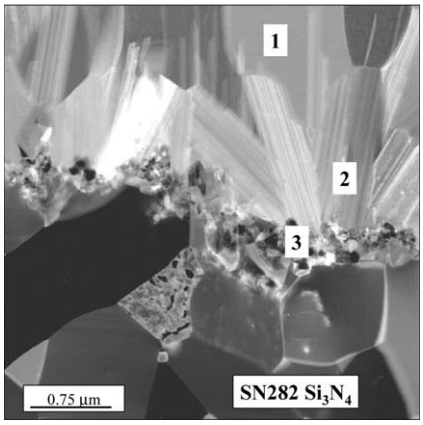

Fig. 4. Cross-section STEM image of the Si_3N_4/coating interface region of the 37Ti–51Al–12Cr coated SN282 coupon after the three, 100 h cycle exposures at 1000 °C in air from Fig. 3. Point 1 exhibited a chemistry of 2Ti:1Al and point 2 a chemistry of 3Ti:1Al. The multiphase, fine-grained region at the coating/Si_3N_4 interface (point 3) was composed of Al–Lu–O and Cr–Si–O rich phases, respectively. No SiO_2 formation at the interface was evident.

was not distinguishable by SEM (Fig. 3), exhibited a composition of ~3Ti:1Al. An additional fine-grained (<0.1 μm), multiphase interfacial layer (point 3) was also identified by STEM analysis adjacent to the Si_3N_4 substrate, which was composed of a Cr–Si–O phase and a Lu–Al–O phase (both Lu and O originate from the lutetium oxide sintering additive already present in the SN282 Si_3N_4). No SiO_2 was identified at the interface, a phase that typically forms on the surface of uncoated Si_3N_4, indicating that the coating layers were protective during the short-term exposures conducted in this study.

The observed microstructural characteristics suggest the following sequence of events. At the onset of oxidation, Al was selectively oxidized from the TiAlCr coating to form Al_2O_3. Concurrently, Ti reacted with the substrate Si_3N_4 to form a Ti-rich nitride. The movement of the Ti to the Si_3N_4 was sufficiently more rapid than the consumption of Al to form Al_2O_3 such that the unusual (and beneficial) situation of Al-enrichment (relative to the initial coating composition) underneath the Al_2O_3 scale resulted. (In TBC/superalloy systems, a major problem is the loss of Al from the bond coat to the substrate superalloy over time at temperature, which ultimately contributes to an inability to maintain Al_2O_3 growth and subsequent coating failure [18,19].) The Cr rejected from the oxidation front and Si moving outwards from the Si_3N_4 reacted with Ti to form a Ti–Si–Cr rich phase as an intermediate layer between the Al-rich outer layer and the Ti-rich inner layer.

The microstructure resulting from the interaction of TiAlCr and Si_3N_4 under oxidizing conditions generally supports the possibility of a self-graded metallic precursor coating, particularly from the standpoint that an Al-rich metallic layer capable of maintaining Al_2O_3-scale formation was formed beneath the growing Al_2O_3 scale. This Al enrichment was critical because, despite the fact the Al_2O_3 remained adherent and protective under the mild thermal cycling conditions used in the present work, cracking of the Al_2O_3 was observed. It was not possible to definitively determine if the cracks were completely through the Al_2O_3 layer, however, the Al-enrichment would permit local re-formation of the Al_2O_3 in the event of such a breach. From a practical standpoint, such behavior may not be acceptable for applications involving frequent on/off thermal cycles (e.g. aircraft engines), but may be tolerable for applications involving long periods of continual operation (primarily isothermal exposures).

The reaction of the Ti with the substrate Si_3N_4 to form a Ti-rich nitride layer at the Si_3N_4 coating interface resulted in an adherent barrier layer that prevented inward migration of the coating constituents to the Si_3N_4 (in the short term exposures conducted). This is important because such inward migration could result in a degradation of the mechanical properties of the Si_3N_4. The formation of the τ phase in the Al-rich layer may also be beneficial from a mechanical property standpoint, as this phase can exhibit plastic deformation at room temperature under compressive loading [17]. However, the formation of the Al–Cr rich intermetallic phase in the Al-rich layer may be problematic, as these phases can exhibit low melting points (below 1200 °C). A key will be how the layered structure evolves with longer term, higher temperature exposures than the simple screening protocol used in the present work. It is interesting to note that at the coupon edge areas, where the TiAlCr coating was on the order of only 2–4 μ thick, the metallic coating was completely consumed to form a mixed Al–Ti–Cr oxide, which remained adherent over the course of the three 100 h cycles. The extent to which partial or complete oxidation of the metallic coating layer is desirable, i.e. the optimal initial coating thickness, remains to be determined. It may also be possible to avoid formation of any low melting point Al-rich phases by modification of the initial coating alloy composition. Detailed studies of the stress state(s) in the layered structures formed by interaction of the metallic coating with Si-based ceramic substrates will also be needed to further evaluate the feasibility of this concept and to guide the design of metallic coating alloys specifically optimized for this application.

4. Summary

(1) An Al_2O_3-forming 37Ti–51Al–12Cr coating on SN282 Si_3N_4 remained adherent over the course of a simple three 100 h cyclic oxidation screening exposure at 1000 °C in air and air + 20% H_2O, without Al_2O_3 scale spallation, despite the CTE mismatches

with the substrate. Cracks were, however, observed at the surface of the Al_2O_3 scale.

(2) The 37Ti–51Al–12Cr coating self graded to form a Ti-rich nitride barrier layer at the coating—Si_3N_4 interface, which had the beneficial and highly unusual consequence of also resulting in Al-enrichment of the alloy underneath the growing Al_2O_3 scale. This enrichment may provide a mechanism for reformation of Al_2O_3 in the event of partial or through thickness scale cracking, as well as a reservoir for extended lifetime. Similar effects may also be of interest to implement in TBC systems to prevent Al loss to the substrate superalloy.

(3) The aforementioned results suggest at least potential feasibility of using metallic alloys as bond coats/protective coatings for Si-based ceramics.

Acknowledgments

The authors thank J.A. Haynes, K.N. Lee, E.J. Opilia, B.A. Pint, and J.L. Smialek for many fruitful discussions in the area of EBCs/TBCs, and T.M. Besmann, R.A. Lowden, and P.F. Tortorelli for reviewing this manuscript. This work was funded by the Assistant Secretary for Energy Efficiency and Renewable Energy For Distributed Energy Programs, United States Department of Energy. Oak Ridge National Laboratory is managed by UT-Battelle, LLC for the US DOE under contract DE-AC05-00OR22725.

References

[1] Opila EJ. J Am Ceram Soc 2003;86(8):1238.
[2] Lee KN, Fox DS, Eldridge JI, Zhu D, Robinson RC, Bansal NP, et al. J Am Ceram Soc 2003;86(8):1299.
[3] Tortorelli PF, More KL. J Am Ceram Soc 2003;86(8):1249.
[4] More KL, Tortorelli PF, Walker LR, Kimmel JB, Miriyala N, Price JR, et al. ASME Paper 2002-GT-30630.
[5] Lin HT, Ferber MK, Westphal W, Macri F. ASME Paper 2002-GT-30629.
[6] Lee KN. Surf Coat Tech 2000;133–134:1.
[7] Eaton HE, Linsey GD, More KL, Kimmel JB, Price JR, Miriyala N. ASME Paper 2000-GT-631.
[8] Ferber MK, Lin HT, Keiser J. ASTM STP 1392. In: Jenkins MG, Lara-Curzio E, Gonczy ST, editors. West Conshohocken, PA: American Society for Testing and Materials; 2000.
[9] Brady MP, Tortorelli PF. Intermetallics 2004;12(7-9):779.
[10] Opila EJ, Myers DL. Alumina volatility in water vapor at elevated temperatures. J Am Ceram Soc, in press.
[11] Nesbitt JA, Vinarcik EJ, Barett CA, Doychak J. Mat Sci Eng A 1992;153:561.
[12] Brady MP, Brindley WJ, Smialek JL, Locci IE. JOM 1996; 8(11):50.
[13] Jewett TJ, Dahms MZ. Metallkunde 1996;87(4):254.
[14] Shao G, Tsakiropoulos P. Intermetallics 1999;7:570.
[15] Lipkin DM, Clarke DR. Oxid Met 1996;45(3–4):267.
[16] Lance MJ, Haynes JA, Cannon WR, Ferber MK. Ceramic transactions: nondestructive evaluation of ceramics; Schilling CH, Gray JN, editors. 1998;89:229.
[17] Klansky JL, Nic JP, Mikkola DE. J Mater Res 1994;6: 255.
[18] Smialek JL, Lowell DE. J Electrochem Soc 1974;121: 800.
[19] Gleeson B, Wang W, Hayashi S, Sordelet D. Mater Sci Forum 2004;461–464:213.